Revisiting Temporal Coupled-Mode Theory in Ultrafast Physics: An Ab-initio Approach

Tong Wu[*1] and *Philippe* Lalanne[*1]

[1] Laboratoire Photonique, Numérique et Nanosciences (LP2N), IOGS- Université de Bordeaux-CNRS, 33400 Talence cedex, France

Abstract. We employ an ab initio Maxwellian approach using quasinormal-mode theory to derive an "exact" Maxwell evolution (EME) equation for resonator dynamics. The new differential equation bears resemblance to the classical one found in coupled-mode-theory (CMT); however, it introduces novel terms embodying distinct physics, suggesting that the CMT predictions could be faulted by dedicated experiments. The new equation is anticipated to be applicable to all electromagnetic resonator geometries, and the theoretical approach we have taken can be extended to other wave physics.

1 Introduction

The temporal coupled-mode theory (CMT) holds the potential to simplify the description of resonant systems with arbitrary material compositions and geometric configurations [1]. At its core, the dynamics of the resonator can be reduced to an ordinary differential equation with respect to time

$$\frac{da_m}{dt} = -i\,\tilde{\omega}_m\,a_m + \langle \kappa_m^* | s_+ \rangle, \tag{1}$$

where $|a_m|^2$ represents the energy stored in the m^{th} mode of the resonator and $\tilde{\omega}_m$ is the complex-valued frequency of the mode, encompassing radiative decay to excitation channels, free space and absorption. We intentionally use conventional notations in Eq. (1) and denote by $|s_+\rangle$ the vector of input amplitudes and $|\kappa_m\rangle$ the vector of coupling constants between the mode and the channels.

Equation (1) stands as a pivotal outcome of CMT, offering high intuitiveness, computational simplicity, and a clear delineation of the physics governing resonances. However, it should be regarded as a heuristic approach, lacking theoretical support for its validity. This work [2] establishes a more rigorous foundation for the CMT evolution, directly from Maxwell equations by employing electromagnetic quasinormal mode (QNM) theory. One significant difference lies in the nature of the driving force: in the EME equation, it is proportional to the derivative of the incident field, while in the CMT. We also elucidate the approximations inherent in the CMT model, comprehend their consequences, and raise awareness when the differences become consequential.

2 The exact Maxwell evolution equation

The EME equation is derived by employing electromagnetic QNM theory, which has now reached a level of maturity that allows its secure application to numerous contemporary electromagnetic challenges in photonics and plasmonics. Electromagnetic QNMs are source-free solutions of Maxwell equations, $\nabla \times \tilde{\mathbf{E}}_m = -i\,\tilde{\omega}_m\,\mu_0\tilde{\mathbf{H}}_m$, $\nabla \times \tilde{\mathbf{H}}_m = i\,\tilde{\omega}_m\varepsilon(\tilde{\omega}_m)\tilde{\mathbf{E}}_m$. $\tilde{\Psi}_m = [\tilde{\mathbf{E}}_m\ \tilde{\mathbf{H}}_m]$ denotes the normalized electric and magnetic fields.

Specifically, QNMs are square-integrable, can undergo normalization, and can be employed to expand the scattered field illuminated by a wavepacket $\mathbf{E}_b(\mathbf{r},t)$ [3]

$$\Psi_S(\mathbf{r},t) = \mathrm{Re}\left(\sum_m \beta_m\,(t)\tilde{\Psi}_m\,(\mathbf{r})\right), \tag{2}$$

where $\beta_m\,(t)$ is the excitation coefficient of the m^{th} mode

$$\beta_m(t) = \int_{-\infty}^{\infty}\left(\int_{-\infty}^{\infty}\frac{\omega}{2\pi(\tilde{\omega}_m-\omega)}O_m(t')\exp\big(i\omega(t'-t)\big)dt'\right)d\omega. \tag{3}$$

Here the overlap is defined as $O_m(t) = \int_{V_r}\Delta\varepsilon(\mathbf{r})\mathbf{E}_b\,(\mathbf{r},t)\cdot\,\tilde{\mathbf{E}}_m\,d^3\,\mathbf{r}$.

The EME equation is derived from Eq. (3) utilizing complex analysis and generalized functions – distributions with a particular emphasis on Cauchy's integral theorem. Another demonstration, which is straightforward, explicit and free of errors, is found in [4].

We recast the temporal integral in Eq. (3) in three terms

$$\beta_m(t) = \int_{-\infty}^{t-\epsilon}\int_{-\infty}^{\infty}\ldots d\omega dt' + \int_{t-\epsilon}^{t+\epsilon}\int_{-\infty}^{\infty}\ldots d\omega\,dt' + \int_{t+\epsilon}^{\infty}\int_{-\infty}^{\infty}\ldots d\omega\,dt' = A + B + C. \tag{4}$$

where the three integrands are strictly identical to that in Eq. (4) and are represented by '…' hereafter. ϵ is a small and positive quantity, and we will consider the limit $\epsilon \to 0$. As $\omega \to \infty$, the exponential factor $\exp(i\omega(t'-t))$ has different behaviors for these three terms.

* Corresponding authors: wutong1121@gmail.com, philippe.lalanne@institutoptique.fr

For term C, we replace the integral path $\int_{-\infty}^{\infty} \ldots d\omega$ with a large semi-circle in the upper complex plane, and it can be shown that its contribution is vanished. For term A, the frequency integral can be replaced by the residue and the large semi-circle in the lower plane. Taking the limit $\epsilon \to 0$, we find $A = i\tilde{\omega}_m \int_{-\infty}^{t} O_m(t') \exp\big(i\tilde{\omega}_m(t'-t)\big)dt'$. For the term B, using the property of the delta function, we can find it is given by $B = -O_m(t)$.

Altogether and upon applying the derivative with respect to t, we obtain the EME equation

$$\frac{d\beta_m(t)}{dt} = -i\tilde{\omega}_m\beta_m(t) - \frac{d}{dt}\langle \mathbf{E}_b(\boldsymbol{r},t)|\Delta\boldsymbol{\varepsilon}(\boldsymbol{r})|\tilde{\mathbf{E}}_m(\boldsymbol{r})\rangle, \quad (5)$$

where $\langle \mathbf{E}_b|\boldsymbol{X}|\tilde{\mathbf{E}}_m\rangle = \int_{V_r} \boldsymbol{X}(\boldsymbol{r})\mathbf{E}_b(\boldsymbol{r},t)\cdot\tilde{\mathbf{E}}_m(\boldsymbol{r})d^3\boldsymbol{r}$.

3 CMT and EME equations comparison

The CMT and EME equations have the following main differences.

- First, the mode excitation by the wavepacket occurs locally in CMT equation, that is s_+ in Eq. (1) is proportional to the wavepacket electric field $\mathbf{E}_b(\mathbf{r}_c,t)$ at an arbitrary point $\mathbf{r}_c$ typically chosen inside the resonator volume. In contrast, the QNM approach predicts a nonlocal excitation that spans the entire resonator volume.
- Second, the driving force is proportional to the derivative of the incident field, which implies that the excitation coefficient β responds instantaneously to the driving field.

We now provide an example to illustrate under which circumstances the difference between results obtained with the CMT and EME formulas can be observed.

For the simulation, we consider a parallelepiped resonator characterized by an isotropic spatially uniform $\Delta\varepsilon$ (see Fig. 1 top). The resonator is assumed to be illuminated by a pulse with an electric field $\mathbf{E}_0\, S(u)\exp(-i\omega u)$, where $u = t-(x-x_c)/c$, $c=1$, $\omega = 1-0.05i$ is a complex frequency and $S(u) = (1+e^{-\rho u})^{-1}$ is the sigmoid function, approaching a Heaviside function for large values of ρ. Note that the carrier frequency ω nearly matches the resonance frequency $\tilde{\omega}_m = 1.1 - 0.0025i$. The pulse is assumed to hint the 'center of coupling' x_c of the resonator at time $t=0$.

Note that with the local approximation and slowly-varying envelop approximation ($\rho \ll 1$), the EME Eq. (5) reduces to the CMT Eq. (1) with $\langle \kappa_m^*|s_+\rangle = i\omega\langle\tilde{\mathbf{E}}_m|\Delta\boldsymbol{\varepsilon}(\boldsymbol{r}_c)|\mathbf{E}_b(\boldsymbol{r}_c,t)\rangle$.

To simplify our qualitative analysis, we also assume that the electric field of the QNM is spatially uniform in the volume $V_r = As$.

Figure 1 (a-c) summarizes the results of a comparison of the predictions obtained with the EME equation Eq. (5) (cyan curve) and Eq. (1) (red curve), for increasing resonator sizes (s) and two pulse shapes (ρ) shown in grey.

We start with a subwavelength resonator ($s = 0.1\lambda$) and a gentle wavefront ($\rho = 0.1$) that resembles a Gaussian pulse. Consistently with other studies (not reported for compactness) with Gaussian pulses, we find a perfect agreement, see Fig. 1a.

To further test the predictive force of Eq. (1), we keep $s = 0.1\lambda$ and consider a steep envelop ($\rho = 1$). Again, we found a remarkable agreement with numerical data obtained directly by solving Eq. (5). This result is not reported in Fig. 1. Then we increase the resonator size ($s = 0.5\lambda$). We observe a discrepancy. However, if we multiply the prediction of Eq. (1) by 0.4, the rescaled data aligns perfectly with the prediction of the EME equation, see Fig. 1b. This is a noteworthy result. The CMT with a fitted coupling constant remains very accurate even when the resonator size is half a wavelength and fast-varying envelopes.

We finally consider a resonator size of one wavelength ($s = 1\lambda$). In this case, even with a large rescaling parameter, the CMT cannot predict the double peak response obtained with the EME equation (Fig. 1c). This implies that, even with fitted coupling coefficients, the CMT equation cannot be accurate and the EME formula emerges as especially important for investigating the fast dynamics of large-sized optical cavities involving linear or nonlinear effects.

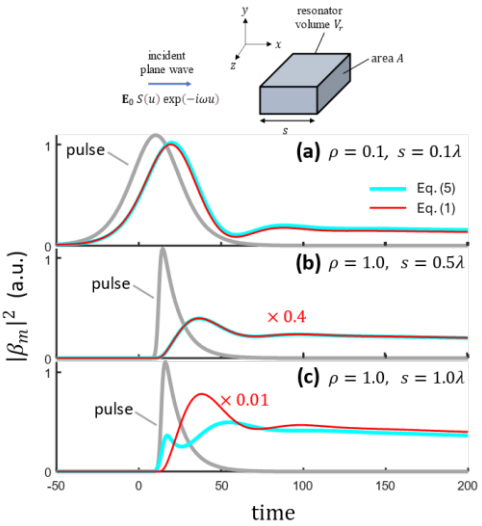

Fig. 1. Comparative analysis of the predictions obtained with the EME Eq. (5) (cyan curves) and the CMT evolution Eq. (1). We consider several resonator sizes ($s = 0.1$,0.5 and 1λ) and pulse shapes ($\rho = 0.1$ and 1) depicted with grey curves for clarity.

References

1. H.A. Haus and W. Huang, Proc. IEEE **79**, 1505 (1991).
2. T. Wu, P. Lalanne, arXiv, 2401.06371 (2024) (accepted in Opt. Express).
3. W. Yan, R. Faggiani, P. Lalanne, Phys. Rev. B **97**, 205422 (2018).
4. R. Zarouf, T. Wu and P. Lalanne, arXiv preprint, arXiv:2405.00455 (2024).